Penerbit Akademia Baru

Progress in Energy and Environment

Journal homepage: http://www.akademiabaru.com/ProgEE.html
ISSN:

Governing Equations in Computational Fluid Dynamics: Derivations and A Recent Review

Review Article

Tey Wah-Yen*[,1,2], Yutaka Asako[2], Nor Azwadi Che Sidik[2], Goh Rui-Zher[1]

[1] Department of Mechanical Engineering, Faculty of Engineering, UCSI University Kuala Lumpur, Kuala Lumpur, Malaysia
[2] Takasago i-Kohza, Department of Mechanical Precision Engineering, Malaysia-Japan International Institute of Technology (MJIIT), Universiti Teknologi Malaysia Kuala Lumpur, Kuala Lumpur, Malaysia

ARTICLE INFO

Article history:
Received 6 April 2017
Received in revised form 27 May 2017
Accepted 27 May 2017
Available online 5 June 2017

Keywords:
Governing equations, Continuum theory, Continuity equations, Navier-Stokes equations, Energy equations

ABSTRACT

The objective of this paper is to provide quick, complete and up-to-date reference on governing equations applied in computational fluid dynamics (CFD) related research, along with the recent review on their future development. The development of non-Newtonian momentum equations, formation of conservation equations in advanced coordinate systems and inclusion of miscellaneous body forces into momentum equations are highlighted. This may ease complicated numerical burdens in solving fluid dynamics equations. Continuity, Navier-Stokes and energy equations are involved, while their coordinate systems span across Cartesian, cylindrical and spherical domain.

1. Introduction

Continuity equations, Navier-Stokes equations and energy equations are the key governing equations that dictate the physics of fluid mechanics and thermal sciences, which are instrumental in the research of computational fluid dynamics (CFD). From simple creeping flow [1,2] and Couette flow [3,4], to the state-of-the-art turbulence modelling [5,6], moving boundaries simulation [7-9], nanofluids motion [10,11], multiphase flow [12,13], complex geometry aerodynamic design [14,15], wave modelling [16,17] and oceanic engineering [18,19], all these engineering researches fall under the purview of these governing equations.

The governing equations stem from the fundamental principles of Newton's Laws and Reynold's transport theorem [20,21], which can be expressed in a general form of integral equations. However, such a general form is not convenient for the precise analysis down to the scale of fluid element parcels [22]. Eulerian approach therefore takes the stage, and it is further developed into the differential form of equations which involve tensors and indicial notation for spatial description and flow fields. Introduction of continuum mechanics and constitutive laws [23,24] had laid down the cornerstone for the derivation of these conservation equations into the governing equations as what we see today.

*Corresponding author.
E-mail address: teywy@ucsiuniversity.edu.my

The general description on the formula in CFD could be found in many textbooks [25-27], yet there is a lack of detailed derivations in a single work with recent reviews. Hence the paper integrates the derivations of these equations with its recent reviews on the essential future development. Section 2 will address the conservative equations, while in Section 3 the development and future research on the conservative equations are highlighted. The development of non-Newtonian momentum equations, formation of conservation equations in advanced coordinate systems and inclusion of miscellaneous body forces into momentum equations are discussed.

2. Governing Equations in CFD

Consider an infinitesimal fluid elements as shown in **Fig. 1** - **3**, which represents the flow field domain based on Cartesian, cylindrical and spherical coordinate respectively. The term $\boldsymbol{\kappa}_{S1,S2}$ is a general representation of flow field vector, in which the subscript S1 and S2 is the spatial component for the flow field vector.

2.1 *Continuity Equations*

Continuity equation can be perceived as nonlinear diffusion equation with regular drift term, and it inspires ubiquitous applications in many fields such as crowd modelling [28], prediction of aerospace debris cloud evolution [29], biomedical imaging [30] and curve measurement analysis [31]. The equation can be treated as either initial boundary problem [32] or Cauchy problem [33] too.

The fundamental physics of Continuity Equations is the principle of conservation of mass, proposed by Lavoisier [34] in 1985. Conservation of mass can be defined as: the conservation law that the rate of change of mass within a control volume (CV) is equivalent to the net rate of mass flowing into the CV [35,36]. Consider the integral form of the mass conservation equation:

$$\frac{\partial}{\partial t}\int_{\mathrm{CV}}\rho.d\mathrm{V}+\int_{\mathrm{CS}}\rho\mathbf{v}.\vec{\mathbf{n}}.d\mathrm{A}=0,\qquad\forall\ \mathbf{v}\in\mathbb{R}\tag{1}$$

Eq. (1) can be transformed to differential form using Gauss' divergence theorem [20,21] to form:

$$\dot{\rho}+\nabla(\rho\mathbf{v})=0\tag{2}$$

However, the paper will demonstrate the derivation approach based on the CV facet analysis. ∇ is the divergence term which can be defined based on its coordinate system, which can be further developed into Eq. (5), (8) or (11).

2.1.1 *Cartesian coordinate Continuity equation*

Consider **Fig. 1**, the length of the infinitesimal fluid element in x, y, and z direction can be assigned as δx, δy and δz respectively. The term $\boldsymbol{\kappa}_{S1,S2}$ in **Fig. 1** can be defined as:

$$\boldsymbol{\kappa}_{S1,S2}=\langle\kappa_{x,x}\quad\kappa_{y,y}\quad\kappa_{z,z}\rangle=\left\{\langle\frac{\partial(\rho u_x)}{\partial x}\quad\frac{\partial(\rho u_y)}{\partial y}\quad\frac{\partial(\rho u_y)}{\partial y}\rangle.V_{\mathrm{car}}\middle|V_{\mathrm{car}}=\delta x\delta y\delta z\right\}\tag{3}$$

The other $\boldsymbol{\kappa}$ are zero due to the non-slip boundary condition and by substituting Eq. (3) into Eq. (1),

$$\frac{\partial\rho}{\partial t}+\frac{\partial(\rho u_x)}{\partial x}+\frac{\partial(\rho u_y)}{\partial y}+\frac{\partial(\rho u_z)}{\partial z}=0\tag{4}$$

Taking $\mathbf{v}=[u_x\quad u_y\quad u_z]$, in an incompressible flow, Eq. (3) will be reduced to $\nabla.\mathbf{v}=0$ where:

$$\nabla=\frac{\partial}{\partial x}+\frac{\partial}{\partial y}+\frac{\partial}{\partial z}\tag{5}$$

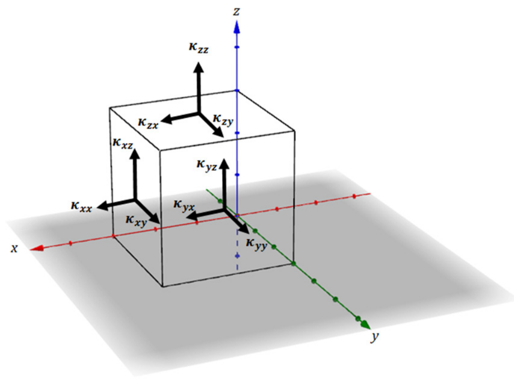

Fig. 1. Infinitesimal fluid field domain based on Cartesian coordinate

2.1.2 *Cylindrical coordinate Continuity equation*

Consider **Fig. 2**, the length of the infinitesimal fluid element in r, θ, and z direction can be assigned as δr, $\delta\theta$ and δz respectively. Upon dimensional expansion, these distances will evolve as $r+\delta r$, $\theta+\delta\theta$ and $z+\delta z$ respectively. The term $\boldsymbol{\kappa}_{S1,S2}$ in **Fig. 2** can be further defined as:

$$\boldsymbol{\kappa}_{S1,S2}=\langle \kappa_{r,r} \quad \kappa_{\theta,\theta} \quad \kappa_{z,z}\rangle=\left\{\langle\frac{\partial(\rho u_r)}{\partial r}+\frac{\rho u_r}{r} \quad \frac{1}{r}\frac{\partial(\rho u_\theta)}{\partial \theta} \quad \frac{\partial(\rho u_z)}{\partial z}\rangle . V_{cyn} \middle| V_{cyn} \approx r\delta\theta\delta r\delta z\right\} \tag{6}$$

The value of other non-normal $\boldsymbol{\kappa}$ is zero too due to the non-slip boundary condition. Note that $\delta r^2 \approx 0$ during the derivation due to its infinite proximity to zero. The volume of the cylinder is:

$$V_{cy}=(\pi(r+\delta r)^2-\pi r^2)\times\frac{\delta\theta}{2\pi}\times\delta z \approx r\delta\theta\delta r\delta z \quad \blacksquare$$

Substitute Eq. (6) into Eq. (1) will yield:

$$\frac{\partial\rho}{\partial t}+\frac{\rho u_r}{r}+\frac{\partial(\rho u_r)}{\partial r}+\frac{1}{r}\frac{\partial(\rho u_\theta)}{\partial \theta}+\frac{\partial(\rho u_z)}{\partial z}=0 \tag{7}$$

If the flow is incompressible, Eq. (7) can be simplified into $\nabla.\mathbf{v} = 0$ too with the divergence term as in Eq. (8), provided that the velocity vector is $\mathbf{v} = [u_r \quad u_\theta \quad u_z]$.

$$\nabla=\frac{1}{r}\frac{\partial(r\ )}{\partial r}+\frac{1}{r}\frac{\partial}{\partial\theta}+\frac{\partial}{\partial z} \tag{8}$$

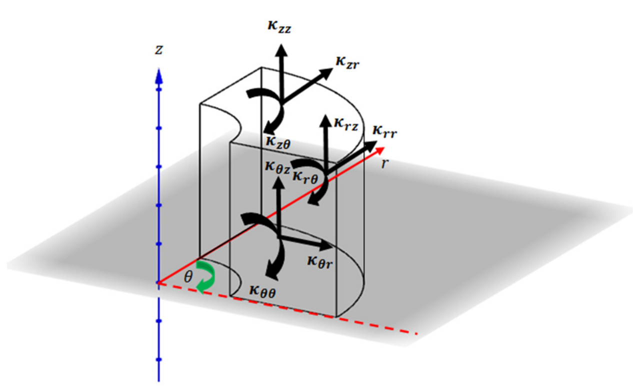

Fig. 2. Infinitesimal fluid field domain based on cylindrical coordinate

2.1.3 *Spherical coordinate Continuity equation*

From **Fig. 3**, the length of control volume boundary and surface of the facets for the spherical fluid element can be shown in **Table 1**. All the $\boldsymbol{\kappa}$ will be zero as well, except $\boldsymbol{\kappa}_{r,r}$, $\boldsymbol{\kappa}_{\theta,\theta}$ and $\boldsymbol{\kappa}_{\phi,\phi}$ which can be mathematically expressed as in Eq. (9).

$$\boldsymbol{\kappa}_{S1,S2}=\langle \kappa_{r,r} \quad \kappa_{\theta,\theta} \quad \kappa_{z,z}\rangle$$
$$=\langle\left(\rho u_r+\frac{\partial(\rho u_r)}{\partial r}\delta r\right)A_{EFGH}-(\rho u_r)A_{ABCD} \quad \left(\rho u_\theta+\frac{\partial(\rho u_\theta)}{\partial\theta}\delta\theta\right).A_{BDFG}-(\rho u_\theta).A_{ACEH} \quad \left(\rho u_\phi+\frac{\partial(\rho u_\phi)}{\partial\phi}\delta\phi\right).A_{CDGH}-(\rho u_\phi).A_{ABEF}\rangle$$
$$=\left\{\langle\frac{\partial(\rho u_r)}{\partial r}+\frac{2\rho u_r}{r} \quad \frac{1}{r}\frac{\partial(\rho u_\theta)}{\partial\theta}+\frac{\rho u_\theta}{r} \quad \frac{\partial(\rho u_\phi)}{\partial\phi}\rangle.V_{sph}\middle| V_{sph}\approx r^2\sin(\theta)\,\delta r\delta\theta\delta\phi\right\} \tag{9}$$

The volume of spherical element can be approximated by taking the product of A_{ACEH} and L_{CD}*, or using the Jacobian rules [37] for the derivation. Substitute Eq. (9) into Eq. (1) will form the compressible Continuity equation as in Eq. (10), in which $\nabla.\mathbf{v}=0$ where $\mathbf{v}=[u_r \quad u_\theta \quad u_\phi]$ will be applied in incompressible case where its divergence term is shown in Eq. (11).

$$\frac{\partial\rho}{\partial t}+\frac{2\rho u_r}{r}+\frac{\partial(\rho u_r)}{\partial r}+\frac{\rho u_\theta}{r}\cot(\theta)+\frac{1}{r}\frac{\partial(\rho u_\theta)}{\partial\theta}+\frac{1}{r\sin(\theta)}\frac{\partial(\rho u_\phi)}{\partial\phi}=0 \tag{10}$$

$$\nabla=\frac{1}{r^2}\frac{\partial(r^2\ )}{\partial r}+\frac{1}{r\sin(\theta)}\frac{\partial(\sin\theta)}{\partial\theta}+\frac{1}{r\sin\theta}\frac{\partial}{\partial\phi} \tag{11}$$

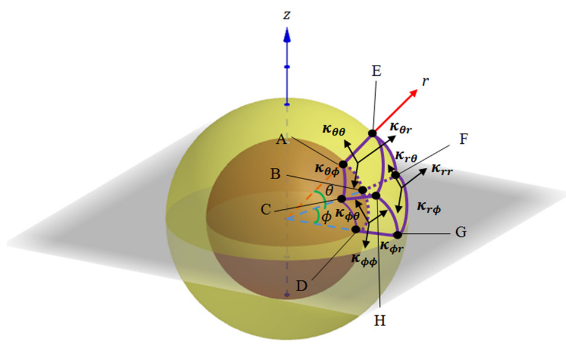

Fig. 3. Infinitesimal fluid field domain based on spherical coordinate

Table 1 Geometry analysis on spherical fluid element based on **Fig. 3**

Geometry	Equation
L_{AB}	$r\delta\theta$
L_{BC}	$r\sin(\theta+\delta\theta)\delta\phi$
L_{CD}	$r\delta\theta$
L_{AD}	$r\sin(\theta)\delta\phi$
L_{EF}	$(r+dr)\delta\theta$
L_{FG}	$(r+\delta r)\sin(\theta+\delta\theta)\delta\phi$
L_{GH}	$(r+\delta r)\delta\theta$
L_{EH}	$(r+\delta r)\sin(\theta)\delta\phi$
L_{AE}, L_{BF}, L_{CG}, L_{DH}	δr
A_{ABCD}	$r^2\sin(\theta)\delta\theta\delta\phi$
A_{EFGH}	$(r+\delta r)^2\sin(\theta)\delta\theta\delta\phi$
A_{BDFG}	$r\sin(\theta+\delta\theta)\delta r\delta\phi$
A_{ACEH}	$r\sin(\theta)\delta r\delta\phi$
A_{ABEF}, A_{CDGH}	$r\delta\theta\delta r$

*$\delta r^2=\delta r^3\approx 0$, $\sin(\delta\theta)\approx\delta\theta$, $\cos(\delta\theta)\approx 1$

2.2 *Navier-Stokes Equations*

Momentum equations are originated from Newton's second law which states that force of a moving object is equivalent to its rate of change of momentum. Expanding the definition will give the momentum equations in a general integral form of [35,38]:

$$\sum \mathrm{F} = \frac{\partial}{\partial t}\int_{\mathrm{CV}} \rho \mathbf{v}.d\mathrm{V} + \int_{\mathrm{CS}} \rho(\mathbf{vv}).\vec{\mathbf{n}}.d\mathrm{A}, \qquad \forall\ \mathbf{v} \in \mathbb{R} \tag{12}$$

The first term of Eq. (12) represents the body forces which may include gravity, Coriolis effects, centrifugal force and electromagnetic force [36]; while the second term denotes the surface forces, which typically refers to pressure force and viscous force. If the flow is in steady state, then $\sum \mathrm{F}$ will be negated. Eq. (12) was expanded by French mathematician Augustin Louis de Cauchy [39] into differential term with the application of divergence theorem in such a way that:

$$\frac{\partial}{\partial t}(\rho \mathbf{v}) + \nabla.(\rho \mathbf{vv}) = \rho \mathrm{g} + \nabla.\overrightarrow{\boldsymbol{\sigma}_{\mathbf{ij}}} \tag{13}$$

$$\frac{\partial}{\partial t}(\rho \mathbf{v}) + \nabla.(\rho \mathbf{vv}) = \rho\left(\frac{\partial \mathbf{v}}{\partial t} + (\mathbf{v}.\nabla)\mathbf{v}\right) = \rho \frac{\mathrm{D}\mathbf{v}}{\mathrm{D}t} \tag{14}$$

Eq. (14) is indeed the material derivative [21], and sometimes it is named as total, particle, Lagrangian, Eulerian or substantial derivatives [26]. It stands for the convection phenomenon and its cancellation implies the formation of creeping flow. ρg and $\nabla.\overrightarrow{\boldsymbol{\sigma}_{\mathbf{ij}}}$ represents body force and sum of applied surface forces, respectively [21]. However, the exact equation for divergence term ∇ will be varied from the coordinate systems. Eq. (13) needs to be further developed, and it will evolve as the famous Navier-Stokes equations [40]. This implies that only Newtonian fluid is considered, while the non-proportional relationship between velocity field and stress tensor which exists in non-Newtonian fluid requires additional modelling [41-44], and it will not be covered in this section.

2.2.1 *Cartesian coordinate Navier-Stokes Equations*

The material derivative of the Cartesian coordinate can be expanded as:

$$\frac{\mathrm{D}\mathbf{v}}{\mathrm{D}t} = \frac{\partial \mathbf{v}}{\partial t} + \frac{\partial \mathbf{v}}{\partial x}\frac{\partial x}{\partial t} + \frac{\partial \mathbf{v}}{\partial y}\frac{\partial y}{\partial t} + \frac{\partial \mathbf{v}}{\partial z}\frac{\partial z}{\partial t} = \frac{\partial \mathbf{v}}{\partial t} + \mathrm{u}_x\frac{\partial \mathbf{v}}{\partial x} + \mathrm{u}_y\frac{\partial \mathbf{v}}{\partial y} + \mathrm{u}_z\frac{\partial \mathbf{v}}{\partial z} \tag{15}$$

The $\boldsymbol{\kappa}_{\mathrm{S1,S2}}$ term in this section refers to viscous forces acting on the control surface of fluid element per unit volume:

$$\boldsymbol{\kappa} = \begin{pmatrix} \kappa_{x,x} & \kappa_{x,y} & \kappa_{x,z} \\ \kappa_{y,x} & \kappa_{y,y} & \kappa_{y,z} \\ \kappa_{z,x} & \kappa_{z,y} & \kappa_{z,z} \end{pmatrix} = \begin{pmatrix} \frac{\partial \tau_{xx}}{\partial x} & \frac{\partial \tau_{xy}}{\partial x} & \frac{\partial \tau_{xz}}{\partial x} \\ \frac{\partial \tau_{yx}}{\partial y} & \frac{\partial \tau_{yy}}{\partial y} & \frac{\partial \tau_{yz}}{\partial y} \\ \frac{\partial \tau_{zx}}{\partial z} & \frac{\partial \tau_{zy}}{\partial z} & \frac{\partial \tau_{zz}}{\partial z} \end{pmatrix} = \frac{\partial \boldsymbol{\tau}}{\partial \mathbf{X}} \tag{16}$$

$$\boldsymbol{\tau} = \begin{pmatrix} \tau_{xx} & \tau_{xy} & \tau_{xz} \\ \tau_{yx} & \tau_{yy} & \tau_{yz} \\ \tau_{zx} & \tau_{zy} & \tau_{zz} \end{pmatrix} = \begin{pmatrix} 2\mu\frac{\partial \mathrm{u}_x}{\partial x} + \lambda\nabla.\mathbf{v} & \mu\left(\frac{\partial \mathrm{u}_x}{\partial y} + \frac{\partial \mathrm{u}_y}{\partial x}\right) & \mu\left(\frac{\partial \mathrm{u}_x}{\partial z} + \frac{\partial \mathrm{u}_z}{\partial x}\right) \\ \mu\left(\frac{\partial \mathrm{u}_y}{\partial x} + \frac{\partial \mathrm{u}_x}{\partial y}\right) & 2\mu\frac{\partial \mathrm{u}_y}{\partial y} + \lambda\nabla.\mathbf{v} & \mu\left(\frac{\partial \mathrm{u}_y}{\partial z} + \frac{\partial \mathrm{u}_z}{\partial y}\right) \\ \mu\left(\frac{\partial \mathrm{u}_z}{\partial x} + \frac{\partial \mathrm{u}_x}{\partial z}\right) & \mu\left(\frac{\partial \mathrm{u}_z}{\partial y} + \frac{\partial \mathrm{u}_y}{\partial z}\right) & 2\mu\frac{\partial \mathrm{u}_z}{\partial z} + \lambda\nabla.\mathbf{v} \end{pmatrix} \tag{17}$$

where $\mathbf{X} = [x\ y\ z]$ while λ is the second viscosity of the fluid, which correspond to the viscous effect due to compression or dilatation [45]. Mathematically, λ=2μ/3-n', where n' can be cancelled out when the fluid exists as monatomic gas at low density [46]. When the flow is incompressible, $\nabla.\mathbf{v} = 0$ takes the second viscosity to be ignorable. By combining Eq. (16) and (17) will form:

$$\boldsymbol{\tau} = \langle \mu\nabla^2 u_x \rangle \mathbf{e_x} + \langle \mu\nabla^2 u_y \rangle \mathbf{e_y} + \langle \mu\nabla^2 u_z \rangle \mathbf{e_z} = \left\langle \mu\nabla^2 \mathbf{v} \middle| \nabla^2 = \frac{\partial^2}{\partial x^2} + \frac{\partial^2}{\partial y^2} + \frac{\partial^2}{\partial z^2} \right\rangle \tag{18}$$

With the presence of pressure gradient per unit volume, Eq. (15) and Eq. (18) can be incorporated to form the Navier-Stokes Equations as in Eq. (19).

$$\rho \frac{D\mathbf{v}}{Dt} = -\frac{\partial P}{\partial X} + \mu\nabla^2 \mathbf{v} + \rho g_X \tag{19}$$

2.2.2 *Cylindrical coordinate Navier-Stokes Equations*

The material derivative in cylindrical coordinate can be obtained as in Eq. (20).

$$\because\ u_r \partial t = \partial r\ ,\ u_\theta \partial t = r\partial\theta\ ,\ u_z \partial t = \partial z$$

$$\frac{D\mathbf{v}}{Dt} = \frac{\partial \mathbf{v}}{\partial t} + \frac{\partial \mathbf{v}}{\partial r}\frac{\partial r}{\partial t} + \frac{\partial \mathbf{v}}{\partial \theta}\frac{\partial \theta}{\partial t} + \frac{\partial \mathbf{v}}{\partial z}\frac{\partial z}{\partial t} \Leftrightarrow \frac{\partial \mathbf{v}}{\partial t} + u_r \frac{\partial \mathbf{v}}{\partial r} + \frac{u_\theta}{r}\frac{\partial \mathbf{v}}{\partial \theta} + u_z \frac{\partial \mathbf{v}}{\partial z} \tag{20}$$

Expanding Eq. (20) with respect to its spatial components,

$$\frac{D\mathbf{v}}{Dt} = \frac{\partial(\mathbf{v}.\mathbf{e_X})}{\partial t} + \frac{u_\theta}{r}\frac{\partial(\mathbf{v}.\mathbf{e_X})}{\partial \theta} + u_z \frac{\partial(\mathbf{v}.\mathbf{e_X})}{\partial z}$$

Note that from differential operations in curvilinear coordinates [47,48],

$$\frac{\partial \mathbf{e}_r}{\partial \theta} = \mathbf{e}_\theta \text{ and } \frac{\partial \mathbf{e}_\theta}{\partial \theta} = -\mathbf{e}_r$$

$$\therefore\ \frac{D\mathbf{v}}{Dt} = \left\langle \frac{\partial u_r}{\partial t} + u_r \frac{\partial u_r}{\partial r} + u_\theta \left(\frac{1}{r}\frac{\partial u_r}{\partial \theta} - \frac{u_\theta}{r} \right) + \frac{\partial u_r}{\partial z} \right\rangle \mathbf{e}_r + \left\langle \frac{\partial u_\theta}{\partial t} + u_r \frac{\partial u_\theta}{\partial r} + u_\theta \left(\frac{1}{r}\frac{\partial u_\theta}{\partial \theta} + \frac{u_r}{r} \right) + \frac{\partial u_\theta}{\partial z} \right\rangle \mathbf{e}_\theta + \left\langle \frac{\partial u_z}{\partial t} + u_r \frac{\partial u_z}{\partial r} + u_\theta \left(\frac{1}{r}\frac{\partial u_z}{\partial \theta} \right) + \frac{\partial u_z}{\partial z} \right\rangle \mathbf{e}_r \tag{21}$$

While the stress tensors for the cylindrical fluid elements are:

$$\boldsymbol{\kappa} = \begin{pmatrix} \kappa_{r,r} & \kappa_{\theta,r} & \kappa_{z,r} \\ \kappa_{r,\theta} & \kappa_{\theta,\theta} & \kappa_{z,\theta} \\ \kappa_{r,z} & \kappa_{\theta,z} & \kappa_{z,z} \end{pmatrix} = \begin{pmatrix} \frac{\tau_{rr}}{r} + \frac{\partial \tau_{rr}}{\partial r} & \frac{1}{r}\frac{\partial \tau_{\theta r}}{\partial \theta} & \frac{\partial \tau_{zr}}{\partial z} \\ \frac{\tau_{r\theta}}{r} + \frac{\partial \tau_{r\theta}}{\partial r} & \frac{1}{r}\frac{\partial \tau_{\theta\theta}}{\partial \theta} & \frac{\partial \tau_{z\theta}}{\partial z} \\ \frac{\tau_{rz}}{r} + \frac{\partial \tau_{rz}}{\partial r} & \frac{1}{r}\frac{\partial \tau_{\theta z}}{\partial \theta} & \frac{\partial \tau_{zz}}{\partial z} \end{pmatrix} = \frac{\partial \boldsymbol{\tau}}{\partial \mathbf{X}} \tag{22}$$

Note that $\delta r^2 \approx 0$ during the simplification process. Due to its mathematical nature in curvilinear coordinates [44,45], the stress tensor will be:

$$\boldsymbol{\tau} = \left\langle \frac{\tau_{rr}}{r} + \frac{\partial \tau_{rr}}{\partial r} + \frac{1}{r}\frac{\partial \tau_{\theta r}}{\partial \theta} + \frac{\partial \tau_{zr}}{\partial z} - \frac{\tau_{\theta\theta}}{r} \right\rangle \mathbf{e}_r + \left\langle \frac{\tau_{r\theta}}{r} + \frac{\partial \tau_{r\theta}}{\partial r} + \frac{1}{r}\frac{\partial \tau_{\theta\theta}}{\partial \theta} + \frac{\partial \tau_{z\theta}}{\partial z} + \frac{\tau_{\theta r}}{r} \right\rangle \mathbf{e}_\theta + \left\langle \frac{\tau_{rz}}{r} + \frac{\partial \tau_{rz}}{\partial r} + \frac{1}{r}\frac{\partial \tau_{\theta z}}{\partial \theta} + \frac{\partial \tau_{zz}}{\partial z} \right\rangle \mathbf{e}_z \tag{23}$$

The single deformation rate, ς could be formulated from the material derivatives from Eq. (21) by removing the unsteady term and the velocity vectors prior to the operators, as shown in Eq. (24). The stress tensor, $\boldsymbol{\tau}$ can be consequently transformed into the deformation rate tensor by the summation of the single deformation and inverse of single deformation.

$$\varsigma = \begin{pmatrix} \varsigma_{rr} & \varsigma_{r\theta} & \varsigma_{rz} \\ \varsigma_{\theta r} & \varsigma_{\theta\theta} & \varsigma_{\theta z} \\ \varsigma_{zr} & \varsigma_{z\theta} & \varsigma_{zz} \end{pmatrix} = \begin{pmatrix} \frac{\partial u_r}{\partial r} & \frac{1}{r}\frac{\partial u_r}{\partial \theta} - \frac{u_\theta}{r} & \frac{\partial u_r}{\partial z} \\ \frac{\partial u_\theta}{\partial r} & \frac{1}{r}\frac{\partial u_\theta}{\partial \theta} + \frac{u_r}{r} & \frac{\partial u_\theta}{\partial z} \\ \frac{\partial u_z}{\partial r} & \frac{1}{r}\frac{\partial u_z}{\partial \theta} & \frac{\partial u_z}{\partial z} \end{pmatrix} \tag{24}$$

$$\boldsymbol{\tau}=\begin{pmatrix}\tau_{rr} & \tau_{r\theta} & \tau_{rz}\\ \tau_{\theta r} & \tau_{\theta\theta} & \tau_{\theta z}\\ \tau_{zr} & \tau_{z\theta} & \tau_{zz}\end{pmatrix}=\mu(\varsigma+\varsigma^{-1})=\mu\begin{pmatrix}2\frac{\partial u_r}{\partial r} & \frac{1}{r}\frac{\partial u_r}{\partial\theta}-\frac{u_\theta}{r}+\frac{\partial u_\theta}{\partial r} & \frac{\partial u_r}{\partial z}+\frac{\partial u_z}{\partial r}\\ \frac{\partial u_\theta}{\partial r}+\frac{1}{r}\frac{\partial u_r}{\partial\theta}-\frac{u_\theta}{r} & 2\left(\frac{1}{r}\frac{\partial u_\theta}{\partial\theta}+\frac{u_r}{r}\right) & \frac{\partial u_\theta}{\partial z}+\frac{1}{r}\frac{\partial u_z}{\partial\theta}\\ \frac{\partial u_z}{\partial r}+\frac{\partial u_r}{\partial z} & \frac{1}{r}\frac{\partial u_z}{\partial\theta}+\frac{\partial u_\theta}{\partial z} & 2\frac{\partial u_z}{\partial z}\end{pmatrix}.(\mathbf{e}_r\quad \mathbf{e}_\theta\quad \mathbf{e}_z) \tag{25}$$

Incorporating Eq. (25) with Eq. (23) will form the cylindrical Navier-Stokes Equation.

$$\boldsymbol{\tau}=\left\{\left\langle\mu\left(\nabla^2u_r-\frac{u_r}{r^2}-\frac{2}{r^2}\frac{\partial u_\theta}{\partial\theta}\right)\right\rangle\mathbf{e}_r+\left\langle\mu\left(\nabla^2u_\theta-\frac{u_\theta}{r^2}+\frac{2}{r^2}\frac{\partial u_r}{\partial\theta}\right)\right\rangle\mathbf{e}_\theta+\langle\mu\nabla^2u_z\rangle\mathbf{e}_z\,\middle|\,\nabla^2=\frac{1}{r}\frac{\partial}{\partial r}\left(r\frac{\partial}{\partial r}\right)+\frac{1}{r^2}\frac{\partial^2}{\partial\theta^2}+\frac{\partial^2}{\partial z^2}\right\} \tag{26}$$

$$\therefore\quad \rho\frac{\mathrm{Dv}}{\mathrm{D}t}=\frac{\partial \mathrm{P}}{\partial \mathrm{X}}+\boldsymbol{\tau}_{\mathbf{X}}+\rho \mathrm{g}_{\mathbf{X}} \tag{27}$$

2.2.3 *Spherical coordinate Navier-Stokes Equations*

The derivation procedure for spherical coordinate Navier-Stokes equations basically complies with all the steps as shown from Eq. (20) - (27). Therefore, only key equations and steps are unfolded here.

$$\because\quad u_r\partial t=\partial r\ ,\ u_\theta\partial t=r\partial\theta\ ,\ u_\phi\partial t=r(\sin\theta)\partial\phi$$

$$\frac{\mathrm{Dv}}{\mathrm{Dt}}=\frac{\partial\mathbf{v}}{\partial t}+\frac{\partial\mathbf{v}}{\partial r}\frac{\partial r}{\partial \mathrm{t}}+\frac{\partial\mathbf{v}}{\partial\theta}\frac{\partial\theta}{\partial \mathrm{t}}+\frac{\partial\mathbf{v}}{\partial\phi}\frac{\partial\phi}{\partial \mathrm{t}}\Leftrightarrow\frac{\partial\mathbf{v}}{\partial t}+u_r\frac{\partial\mathbf{v}}{\partial r}+\frac{u_\theta}{r}\frac{\partial\mathbf{v}}{\partial\theta}+\frac{u_\phi}{r\sin\theta}\frac{\partial\mathbf{v}}{\partial\phi} \tag{28}$$

The differential operations in curvilinear coordinates [47,48] for spherical domain are:

$$\frac{\partial\mathbf{e_X}}{\partial\mathbf{X}}=\begin{pmatrix}\frac{\partial\mathbf{e}_r}{\partial r} & \frac{\partial\mathbf{e}_\theta}{\partial r} & \frac{\partial\mathbf{e}_\phi}{\partial r}\\ \frac{\partial\mathbf{e}_r}{\partial\theta} & \frac{\partial\mathbf{e}_\theta}{\partial\theta} & \frac{\partial\mathbf{e}_\phi}{\partial\theta}\\ \frac{\partial\mathbf{e}_r}{\partial\phi} & \frac{\partial\mathbf{e}_\theta}{\partial\phi} & \frac{\partial\mathbf{e}_\phi}{\partial\phi}\end{pmatrix}=\begin{pmatrix}0 & 0 & 0\\ \mathbf{e}_\theta & -\mathbf{e}_r & 0\\ \mathbf{e}_\phi\sin\theta & \mathbf{e}_\phi\cos\theta & -\mathbf{e}_r\sin\theta-\mathbf{e}_\theta\cos\theta\end{pmatrix} \tag{29}$$

$$\therefore\ \frac{\mathrm{Dv}}{\mathrm{D}t}=\left\langle\frac{\partial u_r}{\partial t}+u_r\frac{\partial u_r}{\partial r}+u_\theta\left(\frac{1}{r}\frac{\partial u_r}{\partial\theta}-\frac{u_\theta}{r}\right)+u_\phi\left(\frac{1}{r\sin\theta}\frac{\partial u_r}{\partial\phi}-\frac{u_\phi}{r}\right)\right\rangle\mathbf{e}_r+\left\langle\frac{\partial u_\theta}{\partial t}+u_r\frac{\partial u_\theta}{\partial r}+u_\theta\left(\frac{1}{r}\frac{\partial u_\theta}{\partial\theta}+\frac{u_r}{r}\right)+u_\phi\left(\frac{1}{r\sin\theta}\frac{\partial u_\theta}{\partial\phi}-\frac{u_\phi\cot\theta}{r}\right)\right\rangle\mathbf{e}_\theta+\left\langle\frac{\partial u_\phi}{\partial t}+u_r\frac{\partial u_\phi}{\partial r}+\frac{u_\theta}{r}\frac{\partial u_\phi}{\partial\theta}+u_\phi\left(\frac{1}{r\sin\theta}\frac{\partial u_\phi}{\partial\phi}+\frac{u_r+u_\theta\cot\theta}{r}\right)\right\rangle\mathbf{e}_r \tag{30}$$

The stress tensor is formed based on the momentum conservation principle by referring to **Fig. 3**.

$$\boldsymbol{\tau}=\left\langle\frac{1}{r^2}\frac{\partial(r^2\tau_{rr})}{\partial r}+\frac{1}{r\sin\theta}\frac{\partial(\tau_{\theta r}\sin\theta)}{\partial\theta}+\frac{1}{r\sin\theta}\frac{\partial\tau_{\phi r}}{\partial\phi}-\frac{\tau_{\theta\theta}+\tau_{\phi\phi}}{r}\right\rangle\mathbf{e}_r+\left\langle\frac{1}{r^3}\frac{\partial(r^3\tau_{r\theta})}{\partial r}+\frac{1}{r\sin\theta}\frac{\partial(\tau_{\theta\theta}\sin\theta)}{\partial\theta}+\frac{1}{r\sin\theta}\frac{\partial\tau_{\phi\theta}}{\partial\phi}-\frac{\tau_{r\theta}+\tau_{\phi\phi}\cot\theta-\tau_{\theta r}}{r}\right\rangle\mathbf{e}_\theta+\left\langle\frac{1}{r^3}\frac{\partial(r^3\tau_{r\phi})}{\partial r}+\frac{1}{r\sin\theta}\frac{\partial(\tau_{\theta\phi}\sin\theta)}{\partial\theta}+\frac{1}{r\sin\theta}\frac{\partial\tau_{\phi\phi}}{\partial\phi}-\frac{\tau_{r\phi}+\tau_{\phi\theta}\cot\theta+-\tau_{\phi r}}{r}\right\rangle\mathbf{e}_z \tag{31}$$

The corresponding constitutive relationships will be:

$$\varsigma=\begin{pmatrix}\varsigma_{rr} & \varsigma_{r\theta} & \varsigma_{rz}\\ \varsigma_{\theta r} & \varsigma_{\theta\theta} & \varsigma_{\theta\phi}\\ \varsigma_{\phi r} & \varsigma_{\phi\theta} & \varsigma_{\phi\phi}\end{pmatrix}=\begin{pmatrix}\frac{\partial u_r}{\partial r} & \frac{1}{r}\frac{\partial u_r}{\partial\theta}-\frac{u_\theta}{r} & \frac{1}{r\sin\theta}\frac{\partial u_r}{\partial\phi}-\frac{u_\phi}{r}\\ \frac{\partial u_\theta}{\partial r} & \frac{1}{r}\frac{\partial u_\theta}{\partial\theta}+\frac{u_r}{r} & \frac{1}{r\sin\theta}\frac{\partial u_\theta}{\partial\phi}-\frac{u_\phi\cot\theta}{r}\\ \frac{\partial u_\phi}{\partial r} & \frac{1}{r}\frac{\partial u_\phi}{\partial\theta} & \frac{1}{r\sin\theta}\frac{\partial u_\phi}{\partial\phi}+\frac{u_r+u_\theta\cot\theta}{r}\end{pmatrix} \tag{32}$$

$$\boldsymbol{\tau}=\begin{pmatrix}\tau_{rr} & \tau_{r\theta} & \tau_{r\phi}\\ \tau_{\theta r} & \tau_{\theta\theta} & \tau_{\theta\phi}\\ \tau_{\phi r} & \tau_{\phi\theta} & \tau_{\phi\phi}\end{pmatrix}=\mu\begin{pmatrix}2\frac{\partial u_r}{\partial r} & \frac{1}{r}\frac{\partial u_r}{\partial\theta}-\frac{u_\theta}{r}+\frac{\partial u_\theta}{\partial r} & \frac{1}{r\sin\theta}\frac{\partial u_r}{\partial\phi}-\frac{u_\phi}{r}+\frac{\partial u_\phi}{\partial r}\\ \frac{\partial u_\theta}{\partial r}+\frac{1}{r}\frac{\partial u_r}{\partial\theta}-\frac{u_\theta}{r} & 2\left(\frac{1}{r}\frac{\partial u_\theta}{\partial\theta}+\frac{u_r}{r}\right) & \frac{1}{r\sin\theta}\frac{\partial u_\theta}{\partial\phi}-\frac{u_\phi\cot\theta}{r}+\frac{1}{r}\frac{\partial u_\phi}{\partial\theta}\\ \frac{\partial u_\phi}{\partial r}+\frac{1}{r\sin\theta}\frac{\partial u_r}{\partial\phi}-\frac{u_\phi}{r} & \frac{1}{r}\frac{\partial u_\phi}{\partial\theta}+\frac{1}{r\sin\theta}\frac{\partial u_\theta}{\partial\phi}-\frac{u_\phi\cot\theta}{r} & 2\left(\frac{1}{r\sin\theta}\frac{\partial u_\phi}{\partial\phi}+\frac{u_r+u_\theta\cot\theta}{r}\right)\end{pmatrix} \tag{33}$$

$$\boldsymbol{\tau}=\left\{\begin{matrix}\mu\left(\nabla^2 u_r-\frac{2u_r}{r^2}-\frac{2}{r^2}\frac{\partial u_\theta}{\partial\theta}-\frac{2u_\theta\cot\theta}{r^2}-\frac{2}{r^2\sin\theta}\frac{\partial u_\phi}{\partial\phi}\right)\mathbf{e}_r+\mu\left(\nabla^2 u_\theta+\frac{2}{r^2}\frac{\partial u_r}{\partial\theta}-\frac{u_\theta}{(r\sin\theta)^2}-\frac{2\cot\theta}{r^2\sin\theta}\frac{\partial u_\phi}{\partial\phi}\right)\mathbf{e}_\theta \\ +\mu\left(\nabla^2 u_z+\frac{2}{r^2\sin\theta}\frac{\partial u_r}{\partial\phi}-\frac{u_\phi}{(r\sin\theta)^2}-\frac{2\cot\theta}{r^2\sin\theta}\frac{\partial u_\theta}{\partial\phi}\right)\mathbf{e}_z\end{matrix}\middle|\nabla^2=\frac{1}{r^2}\frac{\partial^2(r^2)}{\partial\theta^2}+\frac{1}{r^2\sin\theta}\frac{\partial}{\partial\theta}\left(\sin\theta\frac{\partial}{\partial\theta}\right)+\frac{1}{r^2\sin^2\theta}\frac{\partial^2}{\partial\phi^2}\right\} \quad (34)$$

When the pressure effect and body force effect step in, the spherical Navier-Stokes Equations will be formed in the similar way as in Eq. (27).

2.3 *Energy Equations*

The energy increment rate per unit volume, ΔE consists of kinetic term and internal term, while the net heat flux going into the control volume per unit volume, $\dot{q}$. Referring to **Fig. 1**,

$$\Delta E=\rho\frac{D}{Dt}\left(e+\frac{1}{2}\mathbf{v}^2\right) \quad (35)$$

$$\dot{q}=-\left(\frac{\partial q_x}{\partial x}+\frac{\partial q_y}{\partial y}+\frac{\partial q_z}{\partial z}\right)=\left\{-\nabla.q\middle|\nabla=\frac{\partial}{\partial x}+\frac{\partial}{\partial y}+\frac{\partial}{\partial z}\right\} \quad (36)$$

The work done on the control volume, $\dot{W}$ is the product of wall shear stress or pressure, and the velocity component at a fluid element surface:

$$\dot{W}=\left\{-\nabla\cdot(P\mathbf{v})+\frac{\partial(\boldsymbol{\tau}_\mathbf{X}\mathbf{u}_\mathbf{X})}{\partial\mathbf{X}}+\rho\mathbf{V}\mathbf{g}\middle|\boldsymbol{\tau}_\mathbf{X}\|\mathbf{X}\right\} \quad (37)$$

where $\rho\mathbf{Vg}$ represents the work done by the volume force per unit mass which acts on the fluid such as gravity. The pressure and shear stress components are the effect of surface force while the work done by the moving fluid is analogue to the effect of body force as explained in the previous section.

Combining Eq. (35) - (37):

$$\rho\frac{D}{Dt}\left(e+\frac{1}{2}\mathbf{v}^2\right)=-\nabla.q-\nabla\cdot(P\mathbf{v})+\frac{\partial(\boldsymbol{\tau}_\mathbf{X}\mathbf{u}_\mathbf{X})}{\partial\mathbf{X}}+\dot{Q}_{volume}+\rho\mathbf{V}\cdot\mathbf{g}\Leftrightarrow-\nabla.q-\nabla\cdot(P\mathbf{v})+\mathbf{v}\cdot\mathbf{f}+\mu\Phi+\dot{Q}_{volume}+\rho\mathbf{Vg} \quad (38)$$

$$\mathbf{f}=\left(\frac{\partial\tau_{xx}}{\partial x}+\frac{\partial\tau_{yx}}{\partial y}+\frac{\partial\tau_{zx}}{\partial z}\right)\mathbf{e}_x+\left(\frac{\partial\tau_{xy}}{\partial x}+\frac{\partial\tau_{yy}}{\partial y}+\frac{\partial\tau_{zy}}{\partial z}\right)\mathbf{e}_y+\left(\frac{\partial\tau_{xz}}{\partial x}+\frac{\partial\tau_{yz}}{\partial y}+\frac{\partial\tau_{zz}}{\partial z}\right)\mathbf{e}_z \quad (39)$$

$$\mu\Phi=\left(\tau_{xx}\frac{\partial u_x}{\partial x}+\tau_{yy}\frac{\partial u_y}{\partial y}+\tau_{zz}\frac{\partial u_z}{\partial z}\right)+\tau_{xy}\left(\frac{\partial u_y}{\partial x}+\frac{\partial u_x}{\partial y}\right)+\tau_{yz}\left(\frac{\partial u_z}{\partial y}+\frac{\partial u_y}{\partial z}\right)+\tau_{zx}\left(\frac{\partial u_x}{\partial z}+\frac{\partial u_z}{\partial x}\right) \quad (40)$$

where $\dot{Q}_{volume}$ represents a volumetric heat generation per unit volume. Eq. (38) is the one form of the energy equation. However, we can rewrite it to other forms using the Cauchy momentum equation as in Eq. (13). The Cauchy momentum equation can be rewritten as:

$$\rho\frac{D\mathbf{v}}{Dt}=\rho\mathbf{g}-\nabla P+\mathbf{f}$$

$$\rho\mathbf{V}\frac{D\mathbf{v}}{Dt}=\frac{\rho\mathbf{V}}{2}\frac{D\mathbf{v}^2}{Dt}=\rho\mathbf{Vg}-\mathbf{V}.\nabla P+\mathbf{V}.\mathbf{f} \quad (41)$$

$\because$ Fourier's law, $q=-k\nabla.T$

Subtracting Eq. (41) from Eq. (38),

$$\rho\frac{De}{Dt}=\nabla.(k\nabla.T)-P(\nabla.\mathbf{v})+\mu\Phi+\dot{Q}_{volume} \quad (42)$$

Eq. (42) is another form of the energy equation. Note that the $\rho\mathbf{Vg}$ term is vanished in Eq. (42). However, the potential energy based on $\rho\mathbf{Vg}$ is implicitly included in Eq. (42) since the potential energy is considered in Eq. (41). Continuity equation as in Eq. (2) can be rewritten as

$$\nabla\cdot\mathbf{v}=-\frac{1}{\rho}\frac{D\rho}{Dt} \quad (43)$$

By substituting Eq. (43) into (42), Eq. (41) becomes

$$\rho\left(\frac{\mathrm{D}e}{\mathrm{D}t}+\mathrm{P}\frac{\mathrm{D}\rho^{-1}}{\mathrm{D}t}\right)=\nabla\cdot\left(\mathrm{k}\nabla.T\right)+\mu\Phi+\dot{\mathrm{Q}}_{\mathrm{volume}}$$

$$h=e+\mathrm{P}/\rho$$

$$\rho\frac{\mathrm{D}h}{\mathrm{D}t}=\frac{\mathrm{DP}}{\mathrm{Dt}}+\nabla\cdot\left(\mathrm{k}\nabla.T\right)+\mu\Phi+\dot{\mathrm{Q}}_{\mathrm{volume}} \tag{44}$$

Eq. (44) is the most common form of the energy equation. Expanding viscous tensor, Φ:

$$\Phi=\begin{cases}\left(\frac{\partial u_y}{\partial x}+\frac{\partial u_x}{\partial y}\right)^2+\left(\frac{\partial u_z}{\partial y}+\frac{\partial u_y}{\partial z}\right)^2+\left(\frac{\partial u_x}{\partial z}+\frac{\partial u_z}{\partial x}\right)^2+\frac{2}{3}\left(\left(\frac{\partial u_x}{\partial x}-\frac{\partial u_y}{\partial y}\right)^2+\left(\frac{\partial u_y}{\partial y}-\frac{\partial u_z}{\partial z}\right)^2+\left(\frac{\partial u_z}{\partial z}-\frac{\partial u_x}{\partial x}\right)^2\right) & \text{Cartesian}\\ \left(\frac{\partial u_\theta}{\partial x}-\frac{u_\theta}{r}+\frac{1}{r}\frac{\partial u_r}{\partial\theta}\right)^2+\left(\frac{1}{r}\frac{\partial u_z}{\partial\theta}+\frac{\partial u_\theta}{\partial z}\right)^2+\left(\frac{\partial u_r}{\partial z}+\frac{\partial u_z}{\partial r}\right)^2+2\left(\left(\frac{\partial u_r}{\partial r}\right)^2+\left(\frac{1}{r}\frac{\partial u_\theta}{\partial\theta}+\frac{u_r}{r}\right)^2+\left(\frac{\partial u_z}{\partial z}\right)^2\right)-\frac{2}{3}(\nabla\cdot\mathbf{v})^2 & \text{Cylindrical}\\ \left(r\frac{\partial}{\partial r}\left(\frac{u_\phi}{r}\right)+\frac{1}{r}\frac{\partial u_r}{\partial\phi}\right)^2+\left(\frac{\sin\phi}{r}\frac{\partial}{\partial\theta}\left(\frac{u_\theta}{r\sin\phi}\right)+\frac{1}{r\sin\phi}\frac{\partial u_\theta}{\partial\theta}\right)^2+\left(\frac{1}{r\sin\phi}\frac{\partial u_r}{\partial\theta}+r\frac{\partial}{\partial r}\left(\frac{u_\theta}{r}\right)\right)^2+2\left(\left(\frac{\partial u_r}{\partial r}\right)^2+\left(\frac{1}{r}\frac{\partial u_\phi}{\partial\phi}+\frac{u_r}{r}\right)^2+\left(\frac{1}{r\sin\phi}\frac{\partial u_\theta}{\partial\theta}+\frac{u_r}{r}+\frac{u_\phi\cot\phi}{r}\right)^2\right)-\frac{2}{3}(\nabla\cdot\mathbf{v})^2 & \text{Spherical}\end{cases} \tag{45}$$

The specific enthalpy is a function of temperature and pressure. It can be expressed as

$$\mathrm{d}h=\left(\frac{\partial h}{\partial T}\right)_p\mathrm{d}T+\left(\frac{\partial h}{\partial P}\right)_T\mathrm{d}P \tag{46}$$

The thermodynamic relations give us

$$\left(\frac{\partial h}{\partial T}\right)_p=\mathrm{C}_P\,,\qquad \left(\frac{\partial h}{\partial P}\right)_T=\frac{1-\beta T}{\rho} \tag{47}$$

where C_P is the specific heat at constant pressure and β is the volume expansivity, $\beta=-\frac{1}{\rho}\left(\frac{\partial\rho}{\partial T}\right)_P$. If the fluid is an ideal gas, the volume expansivity is

$$\beta=\frac{1}{T} \tag{48}$$

By substituting Eq. (48) into Eq. (47), the specific enthalpy is expressed as

$$\mathrm{d}h=\mathrm{C}_P\mathrm{d}T \tag{49}$$

By substituting Eq. (49) into Eq. (44), the energy equation for an ideal gas is obtained as:

$$\rho\mathrm{C}_P\frac{\mathrm{D}T}{\mathrm{D}t}=\frac{\mathrm{D}P}{\mathrm{D}t}+\nabla\cdot\left(\mathrm{k}\nabla.T\right)+\mu\Phi+\dot{\mathrm{Q}}_{\mathrm{volume}} \tag{50}$$

If the density of a fluid is constant. The volume expansion of such a constant density fluid is zero:

$$\mathrm{d}h=\mathrm{C}_P\mathrm{d}T+\frac{1}{\rho}\mathrm{d}P \tag{51}$$

By substituting Eq. (51) into Eq. (44),

$$\rho\mathrm{C}_P\frac{\mathrm{D}T}{\mathrm{D}t}=\nabla\cdot\left(\mathrm{k}\nabla.T\right)+\mu\Phi+\dot{\mathrm{Q}}_{\mathrm{volume}} \tag{52}$$

Let's consider a steady ideal gas flow without volume heat generation whose properties are constant except the density. The Cartesian coordinate system is considered for convenience. Using the following dimensionless variables:

$$\mathrm{X}=\frac{x}{\mathrm{L}},\quad \mathrm{Y}=\frac{y}{\mathrm{L}},\quad \mathrm{Z}=\frac{z}{\mathrm{L}},\quad \mathrm{U}_x=\frac{u_x}{u_{ref}},\quad \mathrm{U}_y=\frac{u_y}{u_{ref}},\quad \mathrm{U}_z=\frac{u_z}{u_{ref}}\,,$$

$$\mathrm{P}=\frac{\mathrm{P}}{\rho_{ref}u_{ref}^2}\,,\quad \Theta=\frac{T}{T_{ref}},\quad \mathrm{Re}=\frac{\rho_{ref}u_{ref}\mathrm{L}}{\mu},\quad \mathrm{Ma}=\frac{u_{ref}}{\sqrt{\gamma\mathrm{R}_{gas}\mathrm{T}_{ref}}},\quad \rho^*=\frac{\rho}{\rho_{ref}}$$

The energy equation is expressed as

$$\rho^* \left(U_X \frac{\partial\Theta}{\partial X}+U_Y \frac{\partial\Theta}{\partial Y}+U_Z \frac{\partial\Theta}{\partial Z}\right)=(\gamma\text{-}1)Ma^2 \left(U_X \frac{\partial P}{\partial X}+U_Y \frac{\partial P}{\partial Y}+U_Z \frac{\partial P}{\partial Z}\right)+\frac{1}{RePr}\left[\frac{\partial^2\Theta}{\partial X^2}+\frac{\partial^2\Theta}{\partial Y^2}+\frac{\partial^2\Theta}{\partial Z^2}\right]+(\gamma\text{-}1)\frac{Ma^2}{Re}\Phi^* \quad (53)$$

where Φ^* is the dimensionless viscous dissipation function and it can be expressed as:

$$\Phi^*=\left(\left(\frac{\partial U_Y}{\partial X}+\frac{\partial U_X}{\partial Y}\right)^2+\left(\frac{\partial U_Z}{\partial Y}+\frac{\partial U_Y}{\partial Z}\right)^2+\left(\frac{\partial U_X}{\partial Z}+\frac{\partial U_Z}{\partial X}\right)^2\right)+\frac{2}{3}\left(\left(\frac{\partial U_X}{\partial X}-\frac{\partial U_Y}{\partial Y}\right)^2+\left(\frac{\partial U_Y}{\partial Y}-\frac{\partial U_Z}{\partial Z}\right)^2+\left(\frac{\partial U_Z}{\partial Z}-\frac{\partial U_X}{\partial X}\right)^2\right) \quad (54)$$

Note that the first and the third terms of right hand side of Eq. (54) are the substantial derivative of pressure term (SDP) and the viscous dissipation term (VD), respectively. Ma^2 is multiplied to both terms. Therefore, the both SDP and VD terms can be neglected when the Ma of the flow is less than 0.3. However, the both terms should be neglected simultaneously. If one of the both terms remains, this results in physically unrealistic result [49]. Then, the energy equation of an ideal gas flow with low velocity becomes:

$$\rho C_P \frac{DT}{Dt} = \nabla\cdot(k\nabla.T) + \dot{Q}_{volume} \quad (55)$$

The same form of the equation is obtained for a constant density fluid flow if the viscous dissipation is negligible. Usually, the viscous dissipation term for a liquid flow in a conventional size tube is negligible. However, the velocity gradient of a flow in a small sized tube becomes huge, it is to say that the viscous dissipation of a liquid flow in a micro tube whose diameter is less than 200 μm is not negligible [50, 51]. In such a case, Eq. (52) should be solved.

3. Developments and Future Research of CFD Governing Equations

Navier-Stokes equations are the pillar for all the fluid flow dynamics [35], with very wide applications in engineering such as aerodynamics [52-54], fluid-structure interaction [55-60], turbo-machinery [61-64], biomedical simulations [65-68], nanofluids [10,69-71] and bio-inspired transportation [72-75]. Due to its omnipresent applications, providing the solution to the Navier-Stokes Equations becomes one of the largest interests among the researchers. Due to its mathematical perplexity and its application-wise complexity, the equations are solved numerically in three ways: fixed-grid methods [36,40,76-81], immersed boundary methods [82-84], meshfree methods [85-90] and other numerical schemes such as Runge-Kutta method [91,92].

However, Navier-Stokes Equations do not consider many other factors and researches are working on to complement them. Dong and Wu [93] claimed that the current Navier-Stokes Equations have under-estimated the fluid forces, as the rotations, changes in shear rate and turbulence [94] will add in more forces. They modified Eq. (19) to be:

$$\rho \frac{D\mathbf{v}}{Dt}=-\frac{\partial P}{\partial \mathbf{X}}+\mu\nabla^2\mathbf{v}+\rho g_X+f_u^{\ A}+f_u^{\ B}+f_u^{\ R}+f_u^{\ S} \quad (56)$$

where $f_u^{\ A}$, $f_u^{\ B}$, $f_u^{\ R}$ and $f_u^{\ S}$ is additional unsteady force with *u*, additional history force with *u*, additional rotational force with u and additional gradient force, respectively.

The flow is also sometimes associated with a source of vorticity such as pressure gradient due to non-slip boundary conditions and Coriolis effect. Such a flow is named as non-stationary. Ershkov [95,96] modified the Navier-Stokes Equations and developed an approximate solution for it using Riccati partial differential equation [97].

$$0 = -\frac{\partial P}{\partial \mathbf{X}}+\mu\nabla^2\mathbf{v}+\frac{1}{2}(\overrightarrow{u_P}+\overrightarrow{u_W})^2 \quad (57)$$

$\overrightarrow{u_P}$ is the irrotational field of flow while $\overrightarrow{u_W}$ is a solenoidal field of flow velocity which generates a curl field. When the flow becomes turbulent, flow field fluctuation set in and more unknowns transpires. This calls for the necessity to model more equations in order to close the existing equations. Navier-Stokes equations will need to be modified as Reynolds-Averaged Navier-Stokes (RANS) Equations [98,99] as shown in Eq. (59), and therefore turbulence modelling [100-104] is then introduced. Large eddy simulation [105-107] and direct numerical simulation [108-110] are alternatives too to deal with RANS equations.

$$\rho\frac{D\bar{\mathbf{v}}}{Dt}=-\frac{\partial\bar{P}}{\partial X}+\mu\nabla^2\bar{\mathbf{v}}+\rho g_X-\rho\left(\frac{\partial(\overline{\mathbf{v}'.\mathbf{v}'})}{\partial X}\right) \tag{58}$$

Note that $\bar{P}$ and $\bar{\mathbf{v}}$ is the average pressure and velocity respectively, while $\overline{\mathbf{v}'}$ represents the velocity fluctuation. The term $\rho\left(\frac{\partial(\overline{\mathbf{v}'.\mathbf{v}'})}{\partial X}\right)$ is named as Reynolds stress. RANS equations will be significant too at a distance far away from the non-slip wall, as the eddies and turbulence production is high. When the speed of fluid goes beyond unity Mach number, the Navier-Stokes equations need to be modified to fit with the compressible flow [111-113], whereby the second viscosity in Eq. (17) can't be ignored as $\nabla\mathbf{v}\neq 0$.

Meanwhile energy equations are widely applied in computational heat transfer, which is often coupled with the computational fluid dynamics where the Continuity equations and Navier-Stokes equations are applied. Heat transfer analysis for internal flow [114-117], turbo-machinery [119-121] and biological heat transfer [122,123] are amongst the key research areas which needs energy equation as its governing equations.

In short, the development of both Navier-Stokes equations and energy equations move towards the inclusion of more other boundary factors, which re-conciliate the experimental and numerical techniques with the existing equations. Establishment of such ansatz may simplify the procedures in numerical analysis with the reduction of complexity in boundary condition treatment. The future development of the fluid dynamics equations, is not only confined to the solution of the equations using various techniques, but also the improvement of the equations which could predict real phenomenon more accurately. The recommendations for the future development could comprise the development of non-Newtonian momentum equations, formation of conservation equations in advanced coordinate systems and inclusion of more body forces into momentum equations.

3.1 *Development of non-Newtonian Momentum Equations*

Incorporation and simplification of the viscous term for non-Newtonian fluid [124,125]. Although there are a quite number of rheological correlation between the shear stress and viscosity [126-129], the incorporation of the non-Newtonian term into the Navier-Stokes and energy equations will expedite the modelling. This will expand the research horizon into the numerical and algorithm development for solving the engineering problems through computational rheology [130,131].

In this paper, the Ostwald-de Waele power law [132] is taken as the example to be incorporated into momentum equations. By considering the Cartesian coordinate, Eq. (17) can be modified as:

$$\boldsymbol{\tau}=\begin{pmatrix}\mu\left(2\frac{\partial u_x}{\partial x}\right)^n+\lambda\nabla.\mathbf{v} & \mu\left(\frac{\partial u_x}{\partial y}+\frac{\partial u_y}{\partial x}\right)^n & \mu\left(\frac{\partial u_x}{\partial z}+\frac{\partial u_z}{\partial x}\right)^n\\ \mu\left(\frac{\partial u_y}{\partial x}+\frac{\partial u_x}{\partial y}\right)^n & \mu\left(2\frac{\partial u_y}{\partial y}\right)^n+\lambda\nabla.\mathbf{v} & \mu\left(\frac{\partial u_y}{\partial z}+\frac{\partial u_z}{\partial y}\right)^n\\ \mu\left(\frac{\partial u_z}{\partial x}+\frac{\partial u_x}{\partial z}\right)^n & \mu\left(\frac{\partial u_z}{\partial y}+\frac{\partial u_y}{\partial z}\right)^n & \mu\left(2\frac{\partial u_z}{\partial z}\right)^n+\lambda\nabla.\mathbf{v}\end{pmatrix} \tag{59}$$

Substituting Eq. (60) into (19) will lead to Eq. (61):

$$\rho\frac{Du_{\mathbf{X}}}{Dt}=-\frac{\partial P}{\partial\mathbf{X}}+\mu\frac{\partial}{\partial\mathbf{X}}\left(\frac{\partial u_{x_j}}{\partial x_i}+\frac{\partial u_{x_i}}{\partial x_j}\right)^n+\rho g_X \tag{60}$$

where i and j is the spatial component, based on the stress tensor as in Eq. (59). n is the flow behaviour index. If $n < 1$ and $n > 1$ the fluids will exhibit pseudoplastic and dilatant behaviour respectively. The typical example for the former and later fluids is blood plasma and corn starch in ethylene glycol [133]. Eq. (61) can be therefore be applied to solve through various numerical methods such as SIMPLE algorithm [36] and stream-vorticity functions [76].

There are quite a number of non-Newtonian models, which can be found in several textbooks [41,124,125,134-136], which can be indeed further incorporated into the momentum equations. Furthermore, the expansion of the equations into curvilinear coordinate will open up a room for further researches. Such incorporation will path the way for the numerical simulation on non-Newtonian fluids and its conciliation with experimental results. Such development will bridge the gap that many non-Newtonian fluids applications such as blood flow [137-139], food processing [140-142] and chemical reactors [143-145] are simulated based the Stokes Law most of the time.

3.2 *Formation of Conservation Equations in Advanced Coordinate Systems*

Several meshing techniques are proposed in order to deal with the meshing issue. One of them is hybrid meshing [146] which combines the structured, unstructured and chimera grids in order to conform with the problem domain, as shown in **Fig. 4**. Such hybrid meshing calls for great energy when the boundary is in curvature form, while poses potential errors that lead to inconsistency and inaccuracy, including improper skewness, wrap angle ad aspect ratio. Local refinement at the boundary is possible, yet it will consume heavier computational effort.

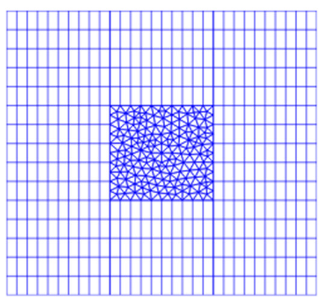

Fig. 4. Hybrid meshing [147]

Some other more sophisticated methods of meshing are proposed too such as medial axis transform [148], all-quad meshing [149], dual contouring tetrahedral decomposition [150], high order curvilinear meshing [151] and radial basis function mesh deformation [152].

To enhance the room for computation without the cost of complex meshing, the Continuity equation, Navier-Stokes equations and energy equations in more advanced coordinate system can be developed. The possible system of coordinate could comprise ellipsoid, cone, hyperboloid and elliptical-paraboloid coordinate. The coordinate equation for ellipsoid, cone, hyperboloid and elliptical-paraboloid is from Eq. (61.1) - (61.4) respectively.

$$\left(\frac{x}{a}\right)^2 + \left(\frac{y}{b}\right)^2 + \left(\frac{z}{c}\right)^2 = 1 \tag{61.1}$$

$$\left(\frac{x}{a}\right)^2 + \left(\frac{y}{b}\right)^2 - \left(\frac{z}{c}\right)^2 = 0 \tag{61.2}$$

$$\left(\frac{x}{a}\right)^2 + \left(\frac{y}{b}\right)^2 - \left(\frac{z}{c}\right)^2 = 1 \tag{61.3}$$

$$\left(\frac{x}{a}\right)^2+\left(\frac{y}{b}\right)^2-\frac{z}{c}=0 \tag{61.4}$$

a, *b* and *c* is the radius in the *x*-, *y*- and *z*- component respectively. However, the main problems in introducing the curvilinear conservation equations are: (1) mathematical complexity of determining the spatial derivatives during the derivations; and (2) singularity issue when the radius is approaching zero. To prevent the singularity issue, sometimes the curvilinear coordinate equations are not applied, while Cartesian equations will take place with some refinement on the meshing [148-152].

However, this remains a great field to be proceeded to enable to more robust computations without meshing issues for quite a wide range of engineering simulations such as airfoils investigation, shipping hydrodynamics, turbo-machineries flow dynamics and processing reactors simulations.

3.3 *Inclusion of More Body Forces into Momentum Equations*

Addition of more body force components into conservative equations, especially the momentum equations will be the next possible research direction. Most of the time, only gravitational force is considered during the modeling, as shown in Eq. (19) and (37). The introduction of electromagnetic force, Coriolis force, centrifugal force, impact force and vibrating force into the conservative equations will complement the equations, which will bring the CFD research to a greater height in investigating engineering physics. In adherence with the dimensional homogeneity of Eq. (19), the modified Navier-Stokes equations with the inclusion of expression of various body force can be:

$$\frac{Du_X}{Dt}=-\frac{\partial P}{\partial X}+\nu\nabla^2 u_X+\rho\left(g_X+\frac{\bar{\bar{v}}^2}{2}\right)+\frac{q}{V}\left(\vec{E}+\vec{v}\vec{H}\right)+2\rho v_t\omega+\rho r\omega^2+\frac{F_0}{V}\cos(\omega t) \tag{62}$$

where $\bar{\bar{v}}$, V, q, $\vec{E}$, $\vec{v}$, $\vec{H}$,v_t, ω, F_0 and ν is vector moving speed of the control volume, volume of infinitesimal fluid element (m^3), electric charge (Coulombs), electric field (volts per meter), charge velocity (m/s), magnetic field (Tesla), tangential velocity (m/s), radial speed (rad/s), vibrating force (Newton) and kinematic viscosity (m^2/s) respectively.

Do note that the term $\rho\frac{\bar{\bar{v}}^2}{2}$ represents impact force, $\frac{q}{V}(\vec{E}+\vec{v}\vec{H})$ is named as Lorentz force equation which represent the electromagnetic force [153], $2\rho v\omega+\rho r\omega^2$ is the Coriolis force or centrifugal force [154] while $\frac{F_0}{V}\cos(\omega t)$ denotes vibrating effects.

It is noteworthy that due to the complexity in the mechanical vibration, F_0 is subjected to various parameters such as forced vibration, free vibration and damping. This will introduce fluid structure interaction with, in which such inclusion of body force may negate the necessity to implement immersed boundary methods [155] and meshfree methods [156,157] in the numerical solution.

4. Conclusion

The full derivations of Continuity equations, Navier-Stokes equations and energy equations have been structured out with physical explanation, applications and development. Recommendations on the future research in the development of governing equations are illustrated too. Development of non-Newtonian momentum equations, introduction of advanced system of coordinate into conservation equations and incorporation of body forces into the momentum equations will help to bypass the necessity to apply complicated numerical techniques in solving fluid dynamics problems. This will suggest a new path for CFD research in the nearest future.

Acknowledgement

The paper is supported by UCSI University - University Pioneer Scientist Incentive Fund (PSIF) with project code Proj-In-FETBE-038.

References

[1] Stokes, G.G. "On the theories of the internal friction of fluid in motion." *Transactions of the Cambridge Philosophical Society* 8 (1845): 287-319; *Mathematical and Physical Papers* 1 (1845): 75-129.
[2] Joseph, D.D. "Potential flow of viscous fluids: Historical notes." *International Journal of Multiphase Flow* 32 (2006): 285-310.
[3] Couette, M. "Etudes sur le frottment des liquides." *Annales de chimie et de physique* 21 (1890): 433-510.
[4] Taylor, G. "Stability of a viscous liquid contained between two rotating cylinders." *Philosophical Transaction of the Royal Society of London* A223 (1923): 289-343.
[5] Spalart, P.R. "Philosophies and fallacies in turbulence modeling." *Progress in Aerospace Science* 74 (2015): 1-15.
[6] Sun, L., Nappo, C.J., Mahrt, L., Belušic, D., Grisogono, B., Stauffer, D.R., Pulido, M., Staquet, C., Jiang, Q., Pouquet, A., Yagüe, C., Galperin, B., Smith, R.B., Finnigan, J.J., Mayor, S.D., Svensson, G., Grachev, A.A. and Neff W.D. "Review of wave-turbulence interactions in the stable atmospheric boundary layer." *Reviews of Geophysics* 53 (2015): 956-993.
[7] Liu, G.R., Wu, Y.L. and Ding, H. "Meshfree weak-strong (MWS) form method and its application to incompressible flow problems." *International Journal for Numerical Methods in Fluids* 46 (2004): 1025-1047.
[8] Tullio, M.D. and Pascazio, G. "A moving-least-squares immersed boundary method for simulating the fluid-structure interaction of elastic bodies with arbitrary thickness." *Journal of Computational Physics* 325 (2016): 201-225.
[9] Das, R. and Cleary, P.W. "Three-dimensional modelling of coupled flow dynamics, heat transfer and residual stress generation in arc welding processes using the meshfree SPH method." *Journal of Computational Science* 16 (2016): 200-216.
[10] Sidik, N.A.C., Samion, S., Ghaderian, J. and Yazid, M.N.A.W.M. "Recent progress on the application of nanofluids in minimum quantity lubrication machining: A review." *International Journal of Heat and Mass Transfer* 108 (2017): 79-89.
[11] Biharaei, M. "Particle migration in nanofluids: A critical review." *International Journal of Thermal Sciences* 109 (2016): 90-113.
[12] Laleh, A.P., Svrcek, W.Y. and Monnery, W.D. "Design and CFD studies of multiphase separators - A Review." *The Canadian Journal of Chemical Engineering* 90 (2012): 1547-1561.
[13] Wang, Z.B., Chen, R. Wang, H., Zhu, X. and Li, S.Z. "An overview of smoothed particle hydrodynamics for simulating multiphase flow." *Applied Mathematical Modeling* 40 (2016): 9625-9655.
[14] Bai, C.J. and Wang, W.C. "Review of computational and experimental approaches to analysis of aerodynamic performance in horizontal-axis wind turbines (HAWTs)." *Renewable and Sustainable Energy Review* 63 (2016): 506-519.
[15] Zhang, J. Zhou, J. Wei, W. and Deng, Y. "Aerodynamic design of an ultra-low rotating speed geared fan." *Aerospace Science and Technology* 63 (2017): 73-81.
[16] Iannelli, J. "A CFD euler solver from a physical acoustics-convection flux Jacobian decomposition." *International Journal for Numerical Methods in Fluids* 31 (1999): 821-861.
[17] Kessentini, A., Taktak, M., Souf, M.A.B., Bareille, O., Ichchou, M.N., Hadder, M. "Computation of the scattering matrix of guided acoustical propagation by the Wave Finite Element approach." *Applied Acoustics* 108 (2016): 92-100.
[18] Jun, B.H., Park, J.Y., Lee, F.Y., Lee, P.M., Lee, C.M., Kim, K., Lim Y.K. and Oh, J.H. "Development of the AUV 'ISiMI' and a free running test in an Ocean Engineering Basin." *Ocean Engineering* 36 (2009): 2-14.
[19] Yan, B.H. "Review of the nuclear reactor thermal hydraulic research in ocean motions." *Nuclear Engineering and Design* 313 (2017): 370-385.
[20] Sultanian, B.K. "*Control Volume Analysis*." In: Sultanian, B.K. Fluid mechanics: An Intermediate Approach. CRC Press, 2016.
[21] Emanuel, G. "*Conservative Equations*." In: Emanuel, G. Analytical Fluid Dynamics. CRC Press, 2016.
[22] Graelbel W.P. Advanced Fluid Mechanics. Elsevier, 2007.
[23] Moore, R.L. "Foundations of point set theory." *American Mathematical Society Colloquium Publication* 13 (1962).
[24] Charatonik, J.J. History of Continuum Theory. Kluwer Academic Publisher, 1998.
[25] White, F.M. Viscous Fluid Flow, 2nd Ed. McGraw Hill Inc, 1994.
[26] Durst, F. Fluid Mechanics: An Introduction to the Theory of Fluid Flows. Springer, 2008.
[27] Kreyszig, E. Advanced Engineering Mathematics, 10th Ed. John Wiley & Sons Inc, 2011.

[28] Carlier, G. and Laborde, M. "Remarks on continuity equations with nonlinear diffusion and nonlocal drifts." *Journal of Mathematical Analysis and Applications* 444 (2016): 1690-1702.
[29] Letizia, F., Colombo, C. and Lewis, H.G. "Multidimensional extension of the continuity equation method for debris clouds evolution." *Advances in Space Research* 57 (2016): 1624-1640.
[30] Dawood, M., Brune, C., Jiang, X., Buther, F., Burger, M., Schober, O., Schafers, M. and Schafers, K.P. A continuity equation based optical flow method for cardiac motion correction in 3D PET data. Medical Imaging and Augmented Reality, Lecture Notes in Computer Science, 2010.
[31] Stepanov, E. and Trevisan, D. "Three superposition principles: Currents, continuity equations and curves of measurement." *Journal of Functional Analysis* 272 (2017): 1044-1103.
[32] Crippa, G., Donadello, C. and Spinolo, L.V. "Initial boundary value problems for continuity equations with BV coefficients." *Journal of MathematiquesPures et Appliquees* 102 (2014): 79-98.
[33] Bogacheva, V.I., DaPratoc, G., Röcknerd, M. and Shaposhnikova,S.V. "On the uniqueness of solutions to continuity equations." *Journal of Differential Equations* 259 (2015): 3854-3873.
[34] Black, J. and Rey J. "An historical note on the conservation of mass." *Journal of Chemical Education* 52 (1975): 658.
[35] Cengel, Y. and Cimbala, J. Fluid Mechanics: Fundamentals and Applications. McGraw Hill Education, 2014.
[36] Versteeg, H.K. and Malalasekera, W. An Introduction to Computational Fluid Dynamics: The Finite Volume Method. Pearson Prentice Hall, 2007.
[37] Greenberg, M. "*Curves, Surfaces and Volumes*." In: Greenberg, M. Advanced Engineering Mathematics, 2nd Ed. Pearson Education Limited, 2014.
[38] Munson, B.R., Young, D.F. and Okiishi, T.H. Fundamentals of Fluid Mechanics. John Wiley and Sons, 2006.
[39] Lemarecha, C. "Cauchy and the gradient method." *Documenta Mathematica Extra Volume ISMP* (2012): 251-254.
[40] Temam, R. Navier-Stokes Equation: Theory and Numerical Analysis. AMS Chelsea Publishing, 2000.
[41] Chhabra, R.P. "Non-Newtonian fluids: An introduction." In *SERC School-cum-Symposium on Rheology of Complex Fluids*, 2010.
[42] Lu, G., Wang, X.D. and Duan, Y.Y. "A critical review of dynamic wetting by complex fluids: From Newtonian fluids to Non-Newtonian fluids and nanofluids." *Advances in Colloid and Interface Science* 236 (2016): 43-62.
[43] Lin J.R., Chu, L.M., Hung, T.C. and Wang, P.Y. "Derivation of two-dimensional non-Newtonian Reynolds equation and application to power-law film slider bearings: Rabinowitsch fluid model." *Applied Mathematical Modelling* 40 (2016) 8832-8841.
[44] Feng, S. and Chen, Q. "Analysis on non-Newtonian characteristics for Nano-magnetic fluid." *Procedia Engineering* 174 (2017): 1208-1214.
[45] Lieberman, L.N. "The second viscosity of liquids." *Physics Review* 76 (1949): 1415-1422.
[46] Lu, G., Wang, X.D. and Duan, Y.Y. "A critical review of dynamic wetting by complex fluids: From Newtonian fluids to Non-Newtonian fluids and nanofluids." *Advances in Colloid and Interface Scienc*e 236 (2016): 43-62.
[47] Bird, R.B., Stewart, W.E. and Lightfoot, E.N. Transport Phenomena. John Wiley & Sons, 2007.
[48] Schlichting, H. Boundary-layer Theory. McGraw-Hill, New York, 1979.
[49] Burmeister, L.C. Convective Heat Transfer. John Wiley & Sons, 1983.
[50] Celata, G.P., Morini, G.L., Marconi, V., McPhail, S.J. and Zummo, G. "Using viscous heating to determine the friction factor in microchannels - An experimental validation." *Experimental Thermal and Fluid Science* 30 (2006): 725-731.
[51] Kawashima, D. and Asako, Y. "First law analysis for viscous dissipation in liquid flows in micro-channels." *International Journal of Heat and Mass Transfer* 55 (2012): 2244-2248.
[52] Dong, H., Wang, C., Li, S. and Song, X.Z. "Numerical research on segmented flexible airfoils considering fluid-structure interaction." *Procedia Engineering* 99 (2015): 57-66.
[53] Morgado, J., Vizinho, R., Silvestre, M.A.R. and Páscoa, J.C. "XFOIL vs CFD performance predictions for high lift low Reynolds number airfoils." *Aerospace Science and Technology* 52 (2016): 207-214.
[54] Kapsalis, P.C.S.,Voutsinas, S. and Vlachos, N.S. "Comparing the effect of three transition models on the CFD predictions of a NACA0012 airfoil aerodynamics." *Journal of Wind Engineering and Industrial Aerodynamics* 157 (2016): 158-170.
[55] Yang, J., Preidikman, S. and Balaras, E. "A strong coupling scheme for fluid-structure interaction problems in viscous incompressible flows." In: *International Conference on Computational Methods for Coupled Problems in Science and Engineering*, Barcelona, 2005.
[56] Göran S., Wernberg, P.A., Davidson, P. Computational Aspects of Structural Acoustics and Vibration. Computational Aspects of Structural Acoustics and Vibration. SpringerLink, 2009.
[57] Khor, C.Y., Abdullah, M.Z., Lau, C.S. and Azid, I.A. "Recent fluid structure interaction modeling challenges in IC encapsulation - A review." *Microelectronics Reliability* 54 (2014): 1511-1526.
[58] Sotiropolous, F. and Yang, X. "Immersed boundary methods for simulating fluid–structure interaction." *Progress in Aerospace Sciences* 65 (2014): 1-21.
[59] Court, S. and Fournie, M. "A fictitious domain finite element method for simulations of fluid-structure interactions:

The Navier-Stokes equations coupled with a moving solid." *Journals of Fluids and Structures* 55 (2015): 398-408.
[60] Lee, H. and Xu, S. "Fully discrete error estimation for a quasi-Newtonian fluid–structure interaction problem." *Computers and Mathematics with Applications* 71 (2016): 2373-2388.
[61] Rasheed, A., Holdahl, R. Kvamsdal, T. and Akervik, E. "A comprehensive simulation methodology for fluid-structure interaction of offshore wind turbines." *Energy Procedia* 53 (2014): 135-145.
[62] Saeed, M. and Kim, M.H. "Airborne wind turbine shell behavior prediction under various wind conditions using strongly coupled fluid structure interaction formulation." *Energy Conversion and Management* 120 (2016): 217-228.
[63] Wang, L., Quant, R. and Kolios, A. "Fluid structure interaction modelling of horizontal-axis wind turbine blades based on CFD and FEA." *Journal of Wind Engineering and Industrial Aerodynamics* 158 (2016): 11-25.
[64] Brahimi, F. and Ouibrahim, A. "Blade dynamical response based on aeroelastic analysis of fluid structure interaction in turbomachinery." *Energy* 115 (2016): 986-995.
[65] Shishir, S.S., Miah, M.A.K., Islam, A.K.M. and Hasan, A.B.M. "Blood flow dynamics in cerebral aneurysm - A CFD simulation." *Procedia Engineering* 105 (2015): 919-927.
[66] Lin, C.H. and Ferng, Y.M. "Investigating thermal mixing and reverse flow characteristics in a T-junction using CFD methodology." *Applied Thermal Engineering* 102 (2016): 733-741.
[67] Sousa, L.C., Castro, C.F., Antonio, C.C., Sousa, F., Santos, R., Castro, P. and Azevedo, E. "Computational simulation of carotid stenosis and flow dynamics based on patient ultrasound data – A new tool for risk assessment and surgical planning." *Advances in Medical Sciences* 61 (2016): 32-39.
[68] Khalafvand, S.S., Ng, E.Y.K., Zhong, L. and Hung, T.K. "Three-dimensional diastolic blood flow in the left ventricle." *Journal of Biomechanics* 50 (2017): 71-76.
[69] Kamyar, A., Saidur, R. and Hasanuzzaman, M. "Application of Computational Fluid Dynamics (CFD) for nanofluids." *International Journal of Heat and Mass Transfer* 55 (2012): 4104-4115.
[70] Sharma, P., Gupta, R., Wanchoo, R.K. "Hydrodynamic studies on glycol based Al_2O_3 nanofluid flowing through straight tubes and coils." *Experimental Thermal and Fluid Science* 82 (2017): 19-31.
[71] Selimefendigil, F., Oztop, H.F. and Chamkha, A.J. "Fluid-structure-magnetic field interaction in a nanofluid filled lid-driven cavity with flexible side wall." *European Journal of Mechanics B/Fluids* 61 (2017): 77-85.
[72] Chen, W., Wu, Z., Liu, J., Shi, S. and Zhou, Y. "Numerical simulation of batoid swimming." *Journal of Hydrodynamics* 23 (2011): 594-600.
[73] Du, L. and Sun, X. "Effect of flapping frequency on aerodynamics of wing in freely hovering flight." *Computers and Fluids* 117 (2015): 79-87.
[74] Tey, W.Y. and Sidik, N.A.C. "A review: The development of flapping hydrodynamics of body and caudal fin movement fishlike structure." *Journal of Advanced Review on Scientific Research* 8 (2015): 19-38.
[75] Olcay, A.B. and Malazi, M.T. "The effects of a longfin inshore squid's fins on propulsive efficiency during underwater swimming." *Ocean Engineering* 128 (2016): 173-182.
[76] Anderson, J.D. Computational Fluid Dynamics: The Basics with Applications. McGraw Hill, 1995.
[77] Jeong, W. and Seong, J. "Comparison of effects on technical variances of computational fluid dynamics (CFD) software based on finite element and finite volume method." *International Journal of Mechanical Sciences* 78 (2014): 19-26.
[78] Mohamad, A.A. Lattice Boltzman Method. Springer, 2011.
[79] Poursharifi, Z. and Sadeghy, K. "On the use of Lattice Boltzmann method for simulating peristaltic flow of viscoplastic fluids in a closed cavity." *Journal of Non-Newtonian Fluid Mechanics* 342 (2017): 1-15.
[80] Liu, Y. and Zhang, W. "Accuracy preserving limiter for the high-order finite volume method on unstructured grids." *Computers and Fluids* 149 (2017): 88-99.
[81] Kozyrakis, G.V., Delis, A.I. and Kampanis, N.A. "A finite difference solver for incompressible Navier-Stokes flows in complex domain." *Applied Numerical Mathematics* 115 (2017): 275-298.
[82] Peskin, C.S. The Immersed Boundary Method. Acta Numerica, Cambridge University Press, 2002.
[83] Silva, A.L.F., Silveria, A. and Damasceno, J.J.R. "Numerical simulation of two-dimensional flows over a circular cylinder using the immersed boundary method." *Journal of Computational Physics* 189 (2015): 351-370.
[84] Li, Z. and Fevier, J. "A coupled volume of fluid and immersed boundary method for simulating 3D multiphase flows with contact line dynamics in complex geometries." *Chemical Engineering Science* 166 (2017): 28 - 41.
[85] Fries, T.P. and Matthies, H.G. Classification and Overview of Meshfree Methods. Institutfur Wissenschaftliches Rechnen, Technische Universitat, 2004.
[86] Huerta, A., Vidal, Y. and Villon, P. "Pseudo-divergence-free element free Galerkin method for incompressible fluid flow." *Computer Methods in Applied Mechanics and Engineering* 193 (2004): 1119-1136.
[87] Liu, G.R. And Gu, Y.T. An Introduction to Meshfree Methods and Their Programming. Springer, 2005.
[88] Liu, G.R. Meshfree Methods: Moving Beyond the Finite Element Method. CRC Press, Taylor and Francis Group, 2009.
[89] Li, H. and Mulay S.S. Meshless Methods and Their Numerical Properties. CRC Press, Taylor and Francis Group, 2013.

[90] Xiao, T., Qin, T., Lu, Z., Sun, X., Tong, M. and Wang, Z. "Development of a smoothed particle hydrodynamics method and its application to aircraft ditching simulations." *Aerospace Science and Technology* 66 (2017): 28-43.
[91] Sanderse, B. and Koren, B. "Accuracy analysis of explicit Runge-Kutta methods applied to the incompressible Navier-Stokes equations." *Journal of Computational Physics* 231 (2012): 3041-3063.
[92] Kazemi-Kamyab, V., Zuijlen, A.H. and Bijl, H. "Analysis and application of high order implicit Runge–Kutta schemes to collocated finite volume discretization of the incompressible Navier–Stokes equations." *Computers and Fluids* 108 (2015): 107-115.
[93] Dong, S. and Wu, S. "A modified Navier-Stokes equation for incompressible fluid flow." *Procedia Engineering* 126 (2015): 169-173.
[94] Osth, J., Noack, B.R., Krajnovic, S., Barros, D. and Boree, J. "On the need for a nonlinear subscale turbulence term in POD models as exemplified for a high-Reynolds-number flow over an Ahmed body." *Journal of Fluid Mechanics* 747 (2014): 518-544.
[95] Ershkow, A. "A procedure for the construction of non-stationary Riccati-type flows for incompressible 3D Navier-Stokes Equations." *Rendiconti del CircoloMatematico di Palermo* 65 (2016): 73-85.
[96] Ershkow, A. "Non-stationary creeping flows for incompressible 3D Navier–Stokes equations." *European Journal of Mechanics B/Fluids* 61 (2017): 154-159.
[97] Ghomanjani, F. and Khorram, E. "Approximate solution for quadratic Riccati differential equation." *Journal of Taibah University for Science* 11 (2017): 246-250.
[98] Rebollo, T.C. and Lewandowki, R. Mathematical and Numerical Foundations of Turbulence Models and Applications. Springer, 2014.
[99] Kajishima, T. and Taira, K. "*Reynolds-Averaged Navier-Stokes Equations*." In: Kajishima, T. and Taira, K. Computational Fluid Dynamics. Springer, 2016.
[100] Mohammadi, B. and Pironneau, O. Analysis of the K-epsilon model. International Nuclear Information System, 1993.
[101] Eghlimi, A., Kouzoubov, A. and Feltcher, C.A.J. "A new RNG-based two-equation model for predicting turbulent gas particle flows." In: *International Conference on CFD in Mineral and Metal Processing and Power Generation*, 1997.
[102] Wilcox, D.C. "Formulation of the k-ω Turbulence Model Revisited." *AIAA Journal* 46 (2008): 2823-2838.
[103] Menter, F.R., Kuntz, M. and Langtry, R. "Ten Years of Industrial Experience with the SST Turbulence Modelling." In: *Turbulence, Heat and Mass Transfer*, Begell House Incorporation, 2003.
[104] Davidson, L. Fluid Mechanics, Turbulent Flow and Turbulence Modelling. Department of Applied Mechanics, Chalmers University of Technology, 2017.
[105] Pope, S.B. "Ten questions concerning the large-eddy simulation of turbulent flows." *New Journal of Physics* 6 (2004): 35.
[106] Berselli, L.C., Iliescu, T. and Layton, W.J. Mathematics of Large Eddy Simulation of Turbulent Flows. Springer, 2005.
[107] Kempe, T. and Hantsch, A. "Large-eddy simulation of indoor air flow using an efficient finite-volume method." *Building and Environment* 115 (2017): 291-305.
[108] Moin, P. and Mahesh, K. "Direct numerical simulation: A tool in turbulence research." *Annual Review of Fluid Mechanics* 30 (1998): 539-578.
[109] Deen, N.G., Peters, E.A.J.F., Padding, J.T. and Kuipers, J.A.M. "Review of direct numerical simulation of fluid–particle mass, momentum and heat transfer in dense gas–solid flows." *Chemical Engineering Science* 116 (2014): 710-724.
[110] Kutawa, Y. and Kuga, K. "Lattice Boltzmann direct numerical simulation of interface turbulence over porous and rough walls." *International Journal of Heat and Fluid Flow* 61 (2016): 145-157.
[111] Plotnikov, Pavel, Sokołowski and Jan. Compressible Navier-Stokes Equations. Springer, 2012.
[112] Bassi, F. and S. Rebay. "A high-order accurate discontinuous finite element method for the numerical solution of the compressible Navier-Stokes equations." *Journal of Computational Physics* 131 (1997): 267-279.
[113] Bresch, D., Desjardins, B. and Gerard-Varet, D. "On compressible Navier-Stokes equations with density dependent viscosities in bounded domains." *Journal de MathématiquesPures et Appliquées* 87 (2007): 227-235.
[114] Zhu, X.W., Fu, Y.H. and Zhao, J.Q. "A novel wavy-tape insert configuration for pipe heat transfer augmentation." *Energy Conversion and Management* 127 (2016): 140-148.
[115] Nayak, B.B., Chatterjee, D. and Mullick, A.N. "Numerical prediction of flow and heat transfer characteristics of water-fly ash slurry in a 180° return pipe bend." *International Journal of Thermal Sciences* 113 (2017): 100-115.
[116] Harvig, J., Sorensen, K. and Condra, D. J. "On the fully-developed heat transfer enhancing flow field in sinusoidally, spirally corrugated tubes using computational fluid dynamics." *International Journal of Heat and Mass Transfer* 106 (2017): 1051-1062.
[117] Abdollahi, A., Sharma, R.N. and Vatani, A. "Fluid flow and heat transfer of liquid-liquid two phase flow in microchannels: A review." *International Journal of Heat and Mass Transfer* 84 (2017): 66-74.
[119] Antonescu, N. and Stanescu, P.D. "Computational model for a condensing boiler with finned tubes heat exchanger."

Energy Procedia 112 (2017): 555-562.
[120] Berrabah, B. and Aminallah, M. "Effect of Coriolis and centrifugal forces on flow and heat transfer at high rotation number and high density ratio in non-orthogonally internal cooling channel." *Chinese Journal of Aeronautics* 30 (2017): 216-324.
[121] Fagundez, J.L.S., Sari, R.L., Martins, M.E.S. and Salau, N.P.G. "Comparative analysis of different heat transfer correlations in a two- zone combustion model applied on a SI engine fueled with wet ethanol." *Applied Thermal Engineering* 115 (2017): 22-32.
[122] Fu, M., Weng, W., Chen, W. and Luo, N. "Review on modeling heat transfer and thermoregulatory responses in human body." *Journal of Thermal Biology* 62 (2016): 189-200.
[123] Ning, M., Song, M., Pan, D. and Deng, S. "Computational fluid dynamics analysis of convective heat transfer coefficients for a sleeping human body." *Applied Thermal Engineering* 117 (2017): 385-396.
[124] Chhabra, R.P. and Richardson, J.F. Non-Newtonian Flow in the Process Industries. Butterworth-Heinemann, 1999.
[125] Irgens, F. Rheology and Non-Newtonian Fluids. Springer Link, 2014.
[126] Myers, T.G. "Application of non-Newtonian models to thin film flow." *Physical Review E 72* (2005): 066302.
[127] Cherizol, R., Sain, M. and Tjong, J. "Review of non-newtonian mathematical models for rheological characteristics of viscoelastic composites." *Green and Sustainable Chemistry* 5 (2015): 6 - 14.
[128] Lin, J.R., Chu, L.M., Hung, T.C. and Wang, P.Y. "Derivation of two-dimensional non-Newtonian Reynolds equation and application to power-law film slider bearings: Rabinowitsch fluid mode." *Applied Mathematical Modelling* 40 (2016): 8832-8841.
[129] Gao, F., Li, W., Meng, B., Wan, M., Zhang, X. and Han, X. "Rheological law and constitutive model for superplastic deformation of Ti-6Al-4V." *Journal of Alloys and Compounds* 701 (2017): 177-185.
[130] Vaziri, A., Xue, Z., Kamm, R.D. and Mofrad, M.R.K. "A computational study on power-law rheology of soft glassy materials with application to cell mechanics." *Computer Methods in Applied Mechanics and Engineering* 196 (2007): 2965-2971.
[131] Vakamalla, T.R. and Mangadoddy, N. "Rheology-based CFD modeling of magnetite medium segregation in a dense medium cyclone." *Powder Technology* 277 (2015): 275-286.
[132] Ozoe, H. and Churchill, S.W. "Hydrodynamic stability and natural convection in Ostwald-de Waele and Ellis Fluids: The development of a numerical solution." *AIChE Journal* 18 (1972): 1196-1207.
[133] Mott R.L. and Untener J.A. Applied Fluid Mechanics, 7th Ed. Pearson Education Limited, 2016.
[134] Steffe, J.F. Rheological Methods in Food Process Engineering, 2nd Ed. Freeman Press, 1996.
[135] Malkin, A. and Isayev, A.I. Rheology: Concepts, Methods and Applications, 2nd Ed. ChemTec Publishing, 2012.
[136] Rubio-Hernandez, F.J., Gomez-Merino, A.I., del Pino, C. Parras, L., Galindo-Rosales, F.J. and Velazquez-Navarro, J.F. Perspectives in Fundamental and Applied Rheology. Malaga, 2013.
[137] Shishir, S. S., Miah, M. A. K., Islam, A. K. M. S. and Hasan, A. B. M. T. "Blood flow dynamics in cerebral aneurysm - A CFD simulation." *Procedia Engineering* 105 (2015): 919-927.
[138] Botar, C. C., Toth, A. A., Klisuric, O. R., Niciforovic, D. D., Cirilovic, V. A. V. and Till, V. E. "Dynamics simulation and doppler ultrasonography validation of blood behaviour in Abdominal Aortic Aneurysm." *Physica Medica* 37 (2017): 1-8.
[139] Bavo, A. M., Pouch, A. M., Degroote, J., Vierendeels, J., Gorman, J. H., Gorman, R. C. and Segers, P. "Patient-specific CFD models for intraventricular flow analysis from 3D ultrasound imaging: Comparison of three clinical cases." *Journal of Biomechanics* 50 (2017): 144-150.
[140] Keshtkaran, M., Mohammadifar, M. A., Asadi, G. H., Nejad, R. A. and Balaghi, S. "Effect of gum tragacanth on rheological and physical properties of a flavored milk drink made with date syrup." *Journal of Dairy Science* 96 (2013): 4794-4803.
[141] Lapcik, L., Lapcikova, B., Otyepkova, E., Otyeoka, M., Vicek, J., Bunka, F. and Salek, R. N. "Surface energy analysis (SEA) and rheology of powder milk dairy products." *Food Chemistry* 174 (2015): 25-30.
[142] Biswas, N., Cheow, Y.L., Tan, C.P. and Siow, L.P. "Physical, rheological and sensorial properties, and bloom formation of dark chocolate made with cocoa butter substitute (CBS)." *LWT - Food Science and Technology* 82 (2017): 420-428.
[143] Plisson, J.S., de Viguerie, L., Tahroucht, L., Menu, M. and Ducouret, G. "Rheology of white paints: How Van Gogh achieved his famous impasto." *Colloids and Surfaces A: Physiochemical and Engineering Aspects* 428 (2014): 134-141.
[144] Goncalves, D., Marques, R., Graca, B., Campos, A.V., Seabra, J.H.O., Leckner, J. and Westbroek, R. "Formulation, rheology and thermal aging of polymer greases, Part II: Influence of the co-thickener content." *Tribology International* 87 (2015): 171-177.
[145] Luo, W., Zhang, Y. and Cong, P. "Investigation on physical and high temperature rheology properties of asphalt binder adding waste oil and polymer." *Construction and Building Materials* 144 (2017): 13-24.
[146] Tu, J., Yeoh, G. and Liu, C. Computational Fluid Dynamics: A Practical Approach, 2nd Ed. Elsevier, 2013.
[147] Zhu, L., Huang, T.Z. and Li, L. "A hybrid-mesh hybridizable discontinuous Galerkin method for solving the time-harmonic Maxwell's equations." *Applied Mathematical Letters* 68 (2017): 109-116.

[148] Quadros, W.R. "LayTracks 3D: A new approach for meshing general solids using medial axis transform." *Computer-Aided Design* 72 (2016): 102-117.

[149] Rushdi, A.A., Mitchell, S.A., Mahmoud, A.H., Bajaj, C.C. and Ebeida, M.S. "All-quad meshing without cleanup." *Computer-Aided Design* 85 (2017): 83-98.

[150] Rashid, T., Sultana, S. and Audette, M.A. "2-manifold surface meshing using dual contouring with tetrahedral decomposition." *Advances in Engineering Software* 102 (2016): 83-96.

[151] Moxey, D., Ekelschot, D., Keskin, U., Sherwin, S.J. and Peiro, J. "High-order curvilinear meshing using a thermo-elastic analogy." *Computer-Aided Design* 72 (2016): 130-139.

[152] Niu, J., Lei, J. and He, J. "Radial basis function mesh deformation based on dynamic control points." *Aerospace Science and Technology* 64 (2017): 122-132.

[153] Staelin, D.H. Electromagnetics and Applications. Department of Electrical Engineering and Computer Science, Massachusetts Institute of Technology, 2011.

[154] Momoniat, E. "A Reynolds equation modelling Coriolis force effect on chemical mechanical polishing." *International Journal of Non-Linear Mechanics* 92 (2017): 111 - 117.

[155] Mittal, R. and Iaccarino, G. "Immersed Boundary Methods." Annual Reviews of Fluid Mechanics 37 (2005): 239-261.

[156] Tsukanov, I., Shapiro, V. and Zhang, S. "A meshfree method for incompressible fluid dynamics problems." *International Journal for Numerical Methods in Engineering* 58 (2003): 127-158.

[157] Liu, G.R. and Gu, Y.T. An Introduction to Meshfree Methods and Their Programming. Springer, 2005